Egypt. J. Soil Sci. **Vol. 61,** No. 4, pp. 459 - 467 (2021)

Egyptian Journal of Soil Science

http://ejss.journals.ekb.eg/

Assessment of Land-Use Dynamics Effects on Water Erosion : Case of the Bouregreg Subwatershed Upstream of the Tiddas Dam, Morroco.

Hicham Ikraoun [(1)]*, Mohamed El Mderssa [(1)], Fouad Malki [(2)], Laila Nassiri [(1)] and Jamal Ibijbijen [(1)]

[1] *Laboratory of Environment and Valorization of Microbial and Vegetal Resources, Departement of Biology, Faculty of Science, Moulay Ismail Univesity, B.P. 11201, Zitoune Meknes, Morocco.*

[2]*Laboratory of Environment, Societies and Territories, Department of Geography, Faculty of Human and Social Sciences, Ibn Tofail University, B.P 242, Kenitra, Morocco.*

Abstract

This paper aims to assess the impact of land-use evolution on water erosion in the Bouregreg subwatershed upstream of the Tiddas dam in the central Moroccan plateau. The methodology adopted is based on a diachronic study of land use between 1989 and 2019 from Landsat images of 30 m resolution. After the necessary pre-proc8essing, a classification of the images of the area using the Support Vector Machine (SVM) algorithm was performed and validated via the data from the processing of aerial photographs from 1989, Google Earth satellite images at a high resolution from 2019 and field validation outputs. The predictive approach falling under the guidelines for mapping and measuring water erosion processes has been exploited to assess the evolution of potential areas for erosion (PAP/CAR guidelines). The results highlight the forest's regression of 5% during the 30 years and the increase in the stages of degradation, namely the rangeland of 6%. The level of erodibility occupying the subwatershed is high to extreme, totalling 63% of the total area. The high to very high levels of soil protection have experienced a regression in their areas ranging from 30% in 1989 to 18% in 2019. The areas vulnerable to a very high level of erosion have seen an increase from 21% in 1989 to 38% in 2019. These results clearly show the worrying state of the area's vulnerability, and thus, make it possible to provide decision-makers with scientific elements that can guide the planning and implementation of action programmes for the protection of the Tiddas Dam.

Keywords: LandSat, PAP/CAR guidelines, Support Vector Machine, Tiddas Dam, Watershed, Water Erosion.

1. Introduction

The phenomenon of water erosion is the form of soil physical degradation that affects more specifically the Mediterranean regions while causing considerable losses of soil, especially areas characterized by medium to steep slopes (Tadrist et al., 2016;Pautrot, 2012; Armand, 2009). This phenomenon causes enormous economic, environmental and social damage. On the economic level, the repercussions of this form of erosion are manifested by the destruction of road infrastructures and engineering structures and the degradation of the productivity of agricultural land (Ousmana et al., 2017). Socially, water erosion is a factor that pushes the rural population to the movetowards the cities through the deterioration of their agricultural land due to the destruction of the soil structure and the reduction of soil fertility. On the environmental side, the process of erosion transports sediments often laden with contaminants, in addition to pesticides and fertilizers, which are often washed away with the soil particles, polluting water sources, wetlands and lakes downstream (El Hadraoui, 2013).

*Corresponding author e-mail: hichamenfi40@gmail.com.;
Rceived: 14/12/2021; Accepted: 1/3/2022
DOI: 10.21608/ejss.2022.110612.1483

For the evaluation of water erosion, several methods have been developed, namely the Universal Soil Loss Equation (USLE), the Revised Universal Soil Loss Equation (RUSLE), the Land Use Evolution and Impact Assessment Model (LEAM), the Priority Actions Programme/Regional Activity Centre (PAP/CAR). Several researchers have demonstrated this last method's capacity for mapping and modelling soil erosion (El Bouqdaoui et al., 2006; Bachaoui et al., 2007; El Aroussi et al., 2013; Akalai et al., 2014; Lahlaoi et al., 2015; Iaaich et al., 2016; Ousmana et al., 2017; Dallahi et al., 2020). It is a method combining two approaches, namely (i) the predictive approach aimed at determining preliminary hypotheses concerning the erosion risk and will be used in the present study, (ii) the descriptive approach consisting of a qualitative assessment of the current and active processes on a given site, and the final phase of integrating the data from the predictive and descriptive phases (Griesbach et al., 1998). This approach is also widely used because of its low requirement for data measurement (Khalef et al., 2020).

The Oued Bouregreg watershed is delimited between the two watershed of Oued Grou and Oued Beht, and subdivided into five sub-basins based on its five main tributaries: Oued Aguennour, lower and middle Bouregreg, Tabahhart and Ksiksou. The maximum floods generate inflows of about 868 Million of m^3 at the site of the future Tiddas dam at the level of the Middle Bouregreg sub-watershed (HCEFLCD, 2012). This situation undoubtedly gives rise to a deep reflection on the threat of silting of the future Tiddas dam under construction.

The land use in this subwatershed and its evolution over time is a determining component for the evaluation of the degree, dynamics and impact of water erosion in this area. The forest cover of this subwatershed upstream of the future Tiddas dam exceeds 75% of its total area. In this context, the present work is a contribution to the diachronic study of the change in land use at 30-year intervals between 1989 and 2019 in the subwatershed upstream of the Tiddas dam. It also aims to assess the evolution of water erosion phenomena between these dates using Geographic Information System (GIS) tools, spatial remote sensing and the maps produced during the evaluation of the state of land use in the diachronic analysis.

2. Presentation of the study area

The subwatershed (SWS) of the middle Bouregreg (MB) upstream of the future Tiddas dam, the subject of this study, covers an area of 26,724.5 ha and is in the centre of the Bouregreg watershed (Figure 1). According to the climatic data from the nearest weather stations, the average annual rainfall is about 341 mm at the Tiddas station and 715 mm at the Oulmés station (ONCA, 2019). The bioclimate that reigned there is semi-arid to subhumid with a cool winter. The study area overlaps two forests, namely Zitchouéne and Bouregreg. The forest cover is spread over an area of about 19,873 ha, these formations are based on green and cork oak and secondary species. The geological formations are mainly based on shale alternating with hard sandstone (Beuadet, 1969; Aherdan, 1994). The SWS of MB upstream of the Tiddas dam is part of the future natural park of the central plateau where studies are being finalised by the departments in charge of water and forestry.

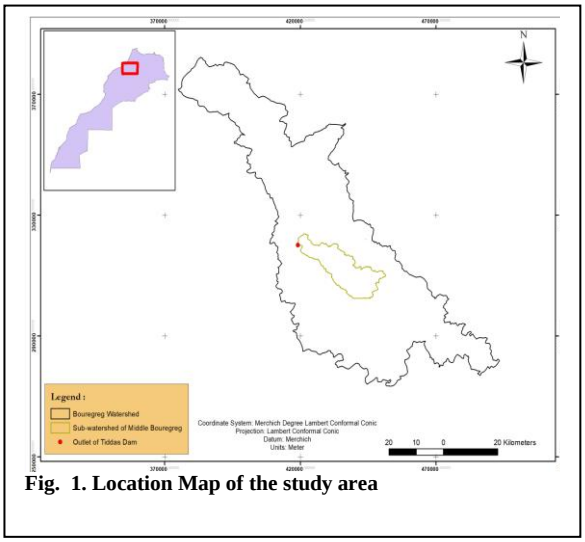

Fig. 1. Location Map of the study area

3. Methodological approach

The land-use mapping and dynamics were based on the Landsat 5 Thematic Mapper (TM) and Landsat 8 Operational Land Imager (OLI) satellite images of 30 m spatial resolution, acquired in 1989 and 2019 – 30 years. The Landsat earth observation programme was chosen for two main reasons: the availability of the images on the United States Geological Survey (USGS) platform free of charge, and the large archive of images over a long period (more than 30 years). The months of the selected images (July and August)

were chosen to minimise cloud cover. The characteristics of these images are listed in Table 1.

After the necessary pre-processing, the classification used for our study is the technique recently applied to the problem of remotely sensing and classifying data using the SVM algorithm (Huang et al., 2002; Zhu and Blumberg, 2002; Schölkopf et al., 2004). This technique represents a promising development in machine learning research with results significantly better in terms of accuracy and generalisation than other traditional algorithms, such as maximum likelihood methods or neural networks (Melgani and Bruzzone, 2004; Pal and Mather, 2005). The goal of the SVM algorithm is to separate all data into two classes by finding the optimal separating function from observations based on known classes of subset data, called the training set (El Malki et al., 2021). The classification was performed on the two Landsat images mentioned above. The quality of this classification was evaluated by calculating the overall accuracy and the Kappa index. This index proposed by Cohen in 1960, is the most widely used index for the evaluation of directed classification (Caloz and Collet, 2001; Dallahi, 2017). As a result of this classification, two land-use maps – 1989 and 2019 – were produced.

To qualitatively and quantitatively assess the trends and changes that occurred during the study period and based on the two land-use maps produced, a land-use change map was generated and statistics on these changes were edited in the form of a Table of Change. The latter map summarises the trend of change over the study period and the table measures these changes in terms of area.

Subsequently, and based on the guidelines of the PAP/RAC predictive approach (Griesbach et al., 1997) summarised in Figure 2, we attempted to map the state of erosion for 1989 and 2019, thus providing a mapping canvas of erosion potential and general trends (Dallahi, 2020). For this purpose, the following elements were used:

- Land-use maps on the two dates were generated in the first step.
- The Digital Terrain Model (DTM) of the subwatershed in question from which the slope map was extracted.
- The geological maps of Morocco 1/50 completed in 2000, which served to identify the substrates present in the subwatershed in question. The latter have been classified according to their degree of soil resistance following the classes dictated in the method PAP/CAR.
- The aerial photographs dating from 1989 to 1990 carried out within the framework of the national forest inventory (NFI), provided a basic platform for the materialisation of the homogeneous areas relating to the degree of ground protection relative to the year 1989.
- Google Earth high-resolution satellite images from 2019.

Table 1. Dates and characteristics of selected LANDSAT images

Satellite	Date	Reference	Nebulosity
Landsat TM 5	15/07/1989	LT05_L1GS_201037_19860808_20180430_01_T2	0 %
Landsat OLI 8	19/08/2019	LC08_L1TP_201037_20190819_20190902_01_T1	1 %

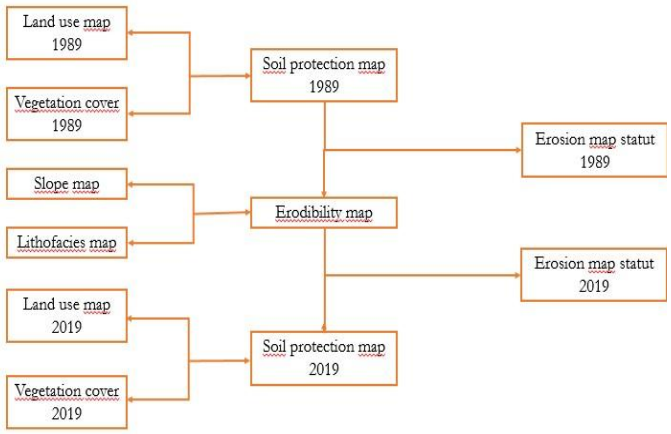

Fig. 2. Methodological flowchart of the application of the method PAP/CAR 1997.

4. Results and Discussions

4.1. Classification results and Land use change analysis

The application of the steps of the above-mentioned classification distinguishes six land use classes: Forest, rangeland, arboriculture, bareland, buildings, and water.

The results of the classification, as well as the parameters for evaluating its quality, are recorded in Figures 3, 4 and 5, and Tables 2 and 3. Thus, this control has allowed us to obtain an overall accuracy of more than 90% for both dates and a value of more than 80% for the Kappa coefficient, thus allowing us to validate the results of this classification. This control has allowed us to obtain a global precision of more than 90% for the two dates, a value higher than 80% for the Kappa coefficient, allowing us to validate the results of this classification (Girard and Girard, 1999).

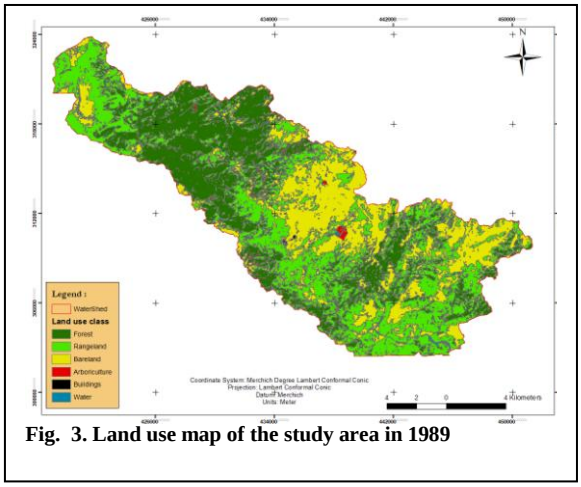

Fig. 3. Land use map of the study area in 1989

The analysis of the land-use change map between 1989 and 2019 in Figure 5 and Table 2 that illustrates the evolution of the areas and that of the change matrix, underlines the study area has undergone changes, thus highlighting a land-use dynamic:

* The forest area has decreased from 8580 ha in 1989 to 7312 ha in 2019, a regression of about 5% with an average of 42 ha/annum. This regression can be explained for different reasons, namely: (i) the severity of climatic conditions, as well as (ii) the strong anthropic pressure due to the absence of other sources of income and the close linkage to the activities of the active population to the peri-forestry and forest areas (HCEFLCD, 2007).

* The rangeland stratum has reported a change in its area of 6% in 2019 compared to 1989, from 10847 ha in 1989 to 12479 ha in 2019.

* The arboriculture land-use class has kept almost the same level, going from 323 ha in 1989 to 291 ha in 2019. Nevertheless, the barelands have experienced a decrease in the area with a percentage of 2.24% in the space of 30 years.

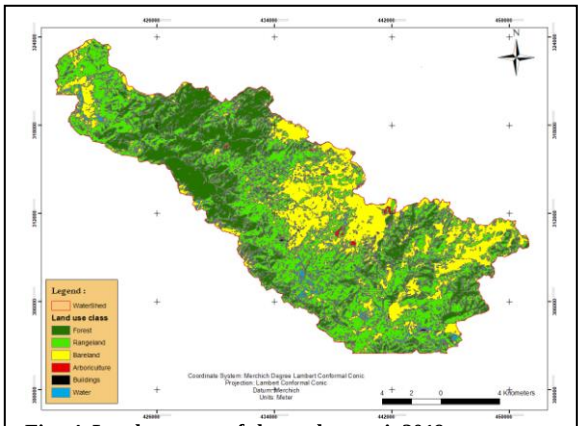

Fig. 4. Land use map of the study area in2019

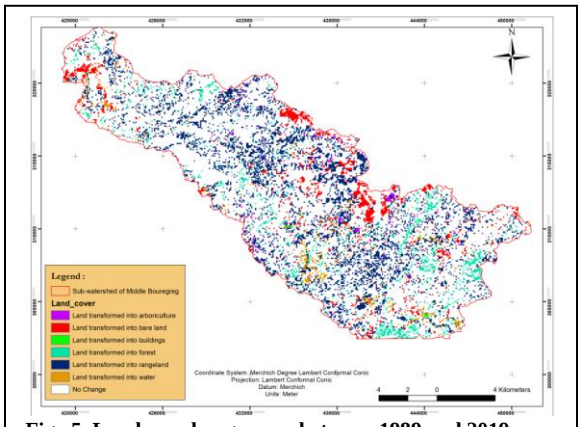

Fig. 5. Land use changes mapbetween 1989 and 2019

4.2. Erodibility map Analysis

The erodibility map is the result of the superposition of the slope and lithofacies maps (Griesbach et al., 1998). The slope map was deduced from the DTM of the subwatershed concerned, and the lithofacies map was elaborated from the geological maps of Morocco 1/50 completed in 2000. The results of this step are shown in Figures 6 and 7

TABLE 2. Evolution of the area of land use between 1989 and 2019

Classes	Area				*Evolution*	
	1989 (ha)	1989 (%)	2019 (ha)	2019 (%)	ha	%
Forest	8580	32,02	7312	27,55	-1268	-4,73
Rangeland	10874	40,58	10997	47,09	1623	6,06
Arboriculture	323	1,21	291	1,10	-32	-0,12
Bare land	6799	25,37	7700	23,36	-599	-2,24
Buildings	26	0,10	34	0,13	8	0,03
Water	195	0,73	462	1,74	267	1,00

TABLE 3. Overallaccuracy and Kappa coefficient

	1989	**2019**
Overall accuracy (%)	93,52	94,77
Kappa coefficient (%)	83,03	85,11

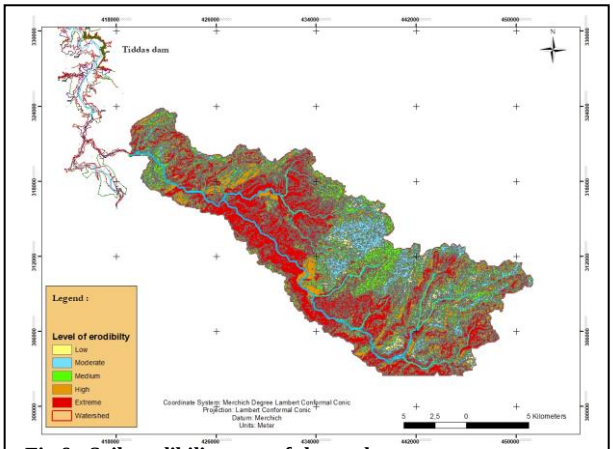

Fig.6 : Soil erodibility map of the study area

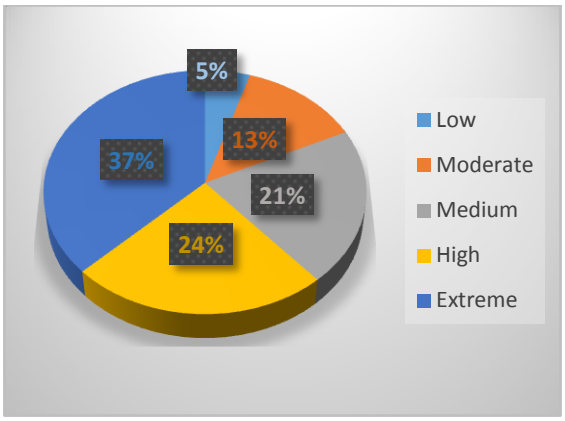

Fig. 7: Differents erodibility's levels of the study area

The analysis of the distribution of erodibility levels (Figures 6 and 7), illustrates the highest being the extreme class with 37% of the total study area, followed by the high erodibility class with 26%. On the other hand, low to moderate erodibility concerns only 18% of the area of the subwatershed studied. These results are consistent with those of the work done by El Hadraoui (2013), on the level of the Bouregreg watershed, where only 13.5% of the basin area is not vulnerable to erosion and about two-thirds of the basin is highly or exceedinglyvulnerable. Erosion is more intense in the Oued Beht river's watershed upstream of the OuljetEssoltane dam. In this last watershed,the erodibility classes that are strong to extreme occupy 83% of the territory, while the low to moderate classes of erodibility occupy only 9% of the surface of this watershed (Ait Yassin et al., 2019).

Additionally, the parts with high to extreme levels of erodibility are mainly located in the Southeast and middle parts of the watershed, which show high slopes. These steep slopes increase the force of rainfall inertia and acceleration (Ait Yassin et al., 2019). Parts of the Southwest and a small area in the middle have low to moderate levels of erodibility, which show low slopes.

4.3. Soilprotection maps analysis

The different types of land cover encountered during the supervised classification of Landsat images in the study area provide a degree of soil protection that corresponds to a specific class. The soil protection map reflects the nature of the occupation and the density of the vegetation cover in the studied subwatershed. For the elaboration of the soil protection map, and to identify the degree of vegetation cover, we used the aerial photographs from 1989 realised within the national forest inventory's (NFI) framework for the year 1989 to 1990, the tools provided by the high-resolution Google Earth 2019 satellite images and field trips. The resulting maps are shown in Figures 8 and 9.

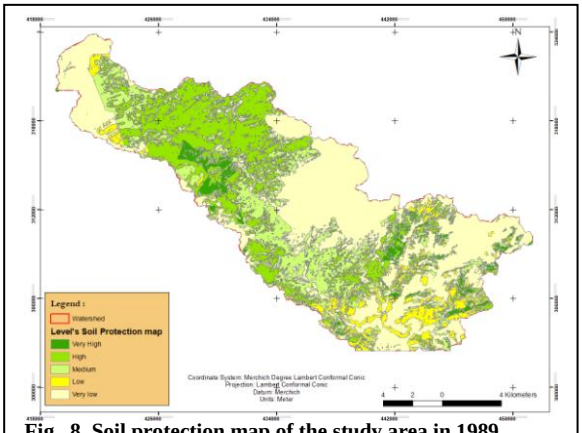

Fig. 8. Soil protection map of the study area in 1989

The results of the diachronic analysis of the soil protection map of the site in question, between 1989 and 2019, show the regressive evolution that the vegetation cover has undergone in terms of area and especially density.

Indeed, we note the increase in the areas of low to verylowsoil protection levels, which have increasedfrom 48% of the total area of the sub-watershedin 1989 to 71% in 2019. In contrast, the high and very high protection levels have evolvedregressivelyfrom 29% in 1989 to 18% in 2019 (Fig. 8 and 9). This regressive change in soil protection levelsis the result of severalfactorsincludingtimberharvesting offenses, overgrazing, and climate change.

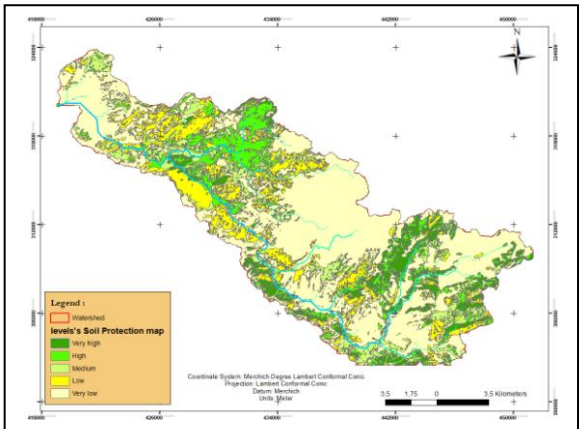

Fig. 9. Soil protection map of the study area in 2019

These findings are similar in terms of the general trend, but less softened for the case study of the Kherouba watershed between 1986 and 2016. An increase in areas of low to very low protection by 7% and regression of high to very high protection levels by 4% was highlighted (Dallahi et al., 2020). This can be explained by the vast area covered by the forest at the Kherouba watershed, which exceeds 87% of its total area, thus providing significant protection against water erosion compared to a rate of forest coverage of 75% at the middle Bouregregsubwatershed level upstream of the Tiddas Dam.

Spatial analysis of the distribution of soil protection levels according to the nature and density of the vegetation cover shows that soils with high protection are mainly located in dense forests with a well-developed undergrowth. On the other hand, soils with low protection are concentrated in cereal crops, bare soils and very degraded rangelands.

4.4. Erosive State Map Analysis

The erosionstatusmap for 1989 and 2019 is the final product of the predictive phase resultingfrom the overlay of the erodibility and soil protection degreemaps. The erosive state maps are recorded in Figures 10 and 11.

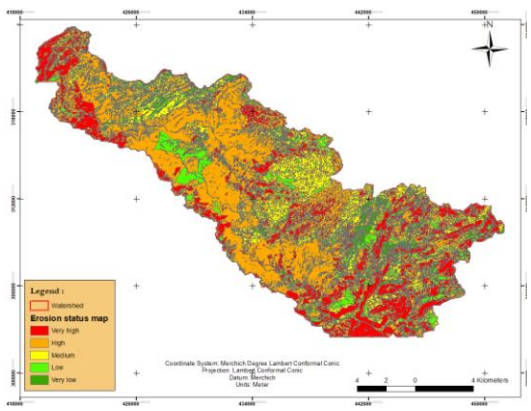

Fig 10. Erosion status map of the study area in 1989

The erosion status map analysis (Figures 10 and 11) shows that only 15% of the area of this subwatershed is at risk of low to very low levels of erosion, while over 46% is at high to extreme levels. It takes different forms of erosion, namely: (i) sheet erosion, which is more or less concentrated due to the phenomenon of runoff and which sometimes exposes the schistose parent rock, (ii) gully erosion, which gives rise to a gully that increases with the aggressiveness and duration of rainfall on unprotected slopes, and (iii) bank undermining at the primary and secondary hydrographic network levels, which is quite dense in the area and is observed during of each flood.

The dynamic of erosion status analysis shows an increase in extreme states from 21% of the total area in 1989 to 38% in 2019. This increase concerns mainly the edges of the Oued Boulhmayel, especially in areas where the vegetation cover has been heavily degraded and where dense forests have been transformed into matorrals. Also, the analysis of the erosive state maps shows that the areas with an important vegetation cover that have not undergone any change have remained barely sensitive to erosion.

These results highlight the preponderant role of vegetation cover in reducing the severity of erosion phenomena. This vegetation protects the soil surface from the impact of raindrops, slows the velocity of runoff water, and maintains good soil porosity making the soil highly resistant to erosion (Sabir et al., 1994; Zhou et al., 2008; Fletcher, 2017; Hou et al., 2016; Dellahi, 2020).

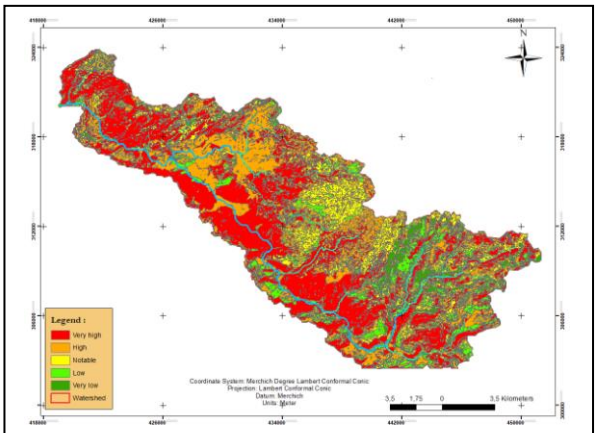

Fig 10. Erosion status map of the study area in 1989

5. Conclusion

The dynamics of land occupations in the sub-watershed of Middle Bouregreg upstream of the future dam of Tiddas has experienced significant changes over the 30 years over the period from 1989 to 2019, especially for the forest component that has experienced a regression of its area of a rate of 5%. This decline is the cause of several factors especially those anthropic which are manifested by the cuts of offences and those relating to the climatic changes through the recurrence of the years of drought and the torrential floods.

This change in the dynamics of land use has highlighted the increase in the risk of water erosion in the study area, which is externalized by the increase in areas vulnerable to water erosion from 21% in 1989 to 38% in 2019.

This situation clearly shows the worrying state of vulnerability of the area, while allowing to provide decision makers with scientific elements that can guide the planning and implementation of action programs for the protection of the future dam of Tiddas under construction.

6. Conflicts of interest

There are no conflicts to declare.

7. Acknowledgments

I would like to thank very much Mr. Amhajer Mohammed and Heyyani Abdelaziz for having provided me with the necessary elements put in their department namely the service of the National Forest Inventory.

8. References

Aherdan, M. (1994) Paysages et évolution du haut-pays du plateau central marocain. Dynamique et propositions d'aménagement (Doctoral dissertation, Université Panthéon-Sorbonne-Paris I).

Ait Yacine, E., Oudija, F., Nassiri, L., Essahlaoui, A. (2019) Modélisation et Cartographie des Risquesd'érosionHydrique du Sol par l'application des SIG, Télédétection et Directives PAP/CAR. Cas du Bassin Versant de Beht, Maroc. *European Scientific Journal*, **15**(12).

Akalai, N., Hlila, R., El Imrani, M., &Darraz, C. (2014) Risk of water erosion in coastalwatershedsnorth of Tetuan (Internel Rif, northern Morocco): Evidences from GIS-based spatial approach. *International Journal of innovation and applied studies*, **8** (4), 1735.

Armand, R. (2009) Étude des états de surface du sol et de leur dynamique pour différentes pratiques de travail du sol. Mise au point d'un indicateur de ruissellement (Doctoral dissertation, Université de Strasbourg).

Bachaoui, B., Bachaoui, E. M., El Harti, A., Bannari, A., & El Ghmari, A. (2007) Cartographie des zones à risque d'érosion hydrique: exemple du haut Atlas marocain. *Télédétection*, **7**(1-2), 3-4.

Beaudet, G. (1969) Le plateau central marocain et ses bordures: étude géomorphologique. Rabat: Imprimeries françaises et marocaines.

Caloz, R., & Collet, C. (2001) Précis de télédétection-Volume 3: Traitements numériques d'images de télédétection (Vol. 3). PUQ.

Dallahi, Y. (2017). Apport de la télédétection spatiale pour l'étude écologique, phytosocio-logique et cartographique de la Tetraclinaie du Site d'Intérêt Biologique et Ecologique (SIBE) de Kharouba (Plateau Central). Faculté des Sciences Mohammed V, Agdal, Rabat, Maroc.

Dallahi, Y., Ouhammou, A., Sbai, M., El Aboudi, A., &Boujraf, A. (2020). Assessment of the vegetation cover change impacts on water erosion, using pap/rac method in upstream of "ouljetsoltane" dam, central plateau-morocco. *Geographia Technica*, **15** (1).

El Aroussi, O., El Garouani, A., &Jabrane, R. (2013) Modelling and mapping of soilerosion on the Oued El Mallehcatchmentusingremotesensing and GIS. *Journal of Urban and Environmental Engineering*, **7**(2), 302-307.

El Hadraoui, Y. (2013) Étude diachronique de l'occupation du sol et de modélisation des processus érosifs du bassin versant du Bouregreg (Maroc) à partir des données de l'Observation de la Terre. Sciences de l'ingénieur.

Elbouqdaoui, K., Ezzine, H., Zahraoui, M., Rouchdi, M., &Badraoui, M. (2006). Évaluation du risque potentiel d'érosion dans le bassin-versant de l'oued Srou (Moyen Atlas, Maroc). *Science et changements planétaires/Sécheresse*, **17**(3), 425-431.

Elmalki, M., Mounir, F., Ichen, A., Khai, T., &Aarab, M. (2021). A diachronicstudy of Ourikawatershed land in the High Atlas of Morocco. In E3S Web of Conferences (Vol. 234). EDP Sciences.

Fletcher, W. J., & Hughes, P. D. (2017). Anthropogenic trigger for lateHolocenesoilerosion in the Jebel toubkal, high Atlas, Morocco. *Catena*, **149**, 713-726.

Girard, M.C., and Girard, M. (1999). Traitement des données de télédétection.

Griesbach, J. C., Ruiz Sinoga, J. D., Giordano, A., Berney, O., Gallart, F., Rojo Serrano, L., &Pavasovic, A. (1998) Guidelines for mapping and measurement of rainfall-inducederosionprocesses in the Mediterranean costal areas.

Haut Commissariat aux Eaux et Forêts et à la Lutte Contre la Désertification 2007, Procès-verbal d'aménagement de la forêt de Bouregreg. Document interne.

Haut Commissariat aux Eaux et Forêts et à la Lutte Contre la Désertification 2012, Procès-verbal d'aménagement du bassin versant d'Oued Bouregreg. Document interne.

Hou, J., Wang, H., Fu, B., Zhu, L., Wang, Y., & Li, Z. (2016). Effects of plant diversity on soilerosion for differentvegetation patterns. *Catena*, **147**, 632-637.

Huang, C., Davis, L. S., & Townshend, J. R. G. (2002). An assessment of support vector machines for land cover classification. *International Journal of remotesensing*, **23**(4), 725-749

Iaaich, H., Moussadek, R., Baghdad, B., Mrabet, R., Douaik, A., Abdelkrim, D., &Bouabdli, A. (2016). Soilerodibility mapping usingthreeapproaches in the Tangiers province–Northern Morocco. *International Soil and Water Conservation Research*, **4**(3), 159-167.

Khallef, B., Mouchara, N., &Brahamia, K. (2020). Cartographie de l'érosion hydrique par l'approche PAP/CAR: Cas du bassin versant d'Oued Bouhamdane (Nord-est de l'Algérie). International Journal of Innovation and *Applied Studies*, **29**(3), 702-716.

Lahlaoi, H., Rhinane, H., Hilali, A., Lahssini, S., &Khalile, L. (2015). Potentialerosionriskcalculationusingremotesensing and GIS in Oued El MalehWatershed, Morocco. *Journal of Geographic Information System*, **7**(02), 128.

Melgani, F., &Bruzzone, L. (2004) Classification of hyperspectral remotesensing images with support vector machines. *IEEE Transactions on geoscience and remotesensing*, **42**(8), 1778-1790.

Ousmana, H., El Hmaidi, A., Essahlaoui, A., Bekri, H., & El Ouali, A. (2017) Modélisation et cartographie du risque de l'érosion hydrique par l'application des SIG et des directives PAP/CAR. Cas du bassin versant de l'Oued Zgane (Moyen Atlas tabulaire, Maroc). *Bulletin de l'Institut Scientifique,* Rabat, Section Sciences de La Terre, **39**, 103-119.

Pal, M., & Mather, P. M. (2005) Support vector machines for classification in remotesensing. *International journal of remotesensing*, **26**(5), 1007-1011.

PAUTROT, C. (2012) Érosion et dégradation des sols. Mémoires de l'Académie nationale de Metz.

Sabir, M., Merzouk, A., &Berkat, O. (1994). Impact du pâturage sur les propriétés hydriques du sol dans un milieu pastoral aride: Aarid, Maroc. *Bulletin du Réseau Érosion*, **14**, 444-462.

Schölkopf, B., Tsuda, K., & Vert, J. P. (2004). Kernel methods in computational biology. MIT press.

Tadrist, N., &Debauche, O. (2016). Impact de l'érosion sur l'envasement des barrages, la recharge des nappes phréatiques côtières et les intrusions marines dans la zone semi-aride méditerranéenne: cas du barrage de Boukourdane (Algérie). *Biotechnologie, Agronomie, Société et Environnement*, **20**(4), 453-467.

Zhou, P., Luukkanen, O., Tokola, T., & Nieminen, J. (2008). Effect of vegetation cover on soilerosion in a mountainouswatershed. *Catena*, **75**(3), 319-325.

Zhu, G., &Blumberg, D. G. (2002). Classification using ASTER data and SVM algorithms: The case study of Beer Sheva, Israel. *Remotesensing of Environment*, **80**(2), 233-240.